Medibots: Dual-Action Biogenic Microdaggers for Single-Cell Surgery and Drug Release

Sarvesh Kumar Srivastava, Mariana Medina-Sánchez, Britta Koch, and Oliver G. Schmidt*

Modern surgery and medicine have witnessed a paradigm shift toward miniaturization of devices thereby attaining improved efficiency as compared to their larger counterparts.[1–3] This has resulted in considerable advancements in the fields of drug delivery,[4,5] diagnostics,[6] minimally invasive surgery (MIS),[7,8] and cell manipulation.[9,10] Micromotors in particular have gained considerable interest owing to their robust miniaturized structure with functional capabilities (e.g., surface chemistry) promoting their application for in vivo administration[11] and improved sensing capabilities,[12] etc. Several studies have been reported where these micromotors have been deployed for cell or analyte capturing and isolation,[13] drug delivery,[14] and tissue-manipulation (drilling into soft materials like tissue).[15,16] Some interesting studies pertaining to biomedical application of micromotors via chemical[17] or physical actuation[18–20] has also been reported. Also, key challenges and opportunities for such micromotors/swimmers in biomedical application have been discussed elsewhere.[21–23]

These microrobots fabricated via microelectromechanical systems (MEMS) technology[24] also highlight the fourth generation of "untethered microsurgeons" much coveted for their small size with the ability to "navigate intracorporeally by penetrating tissue or using anatomical pathways."[25] Most of these microbots are magnetically actuated via an electromagnetic field control due to the miniaturized scaling of electromagnetic forces with respect to the device volume.[26] This is generally achieved by incorporating a layer of ferromagnetic material (like Ni or Fe) allowing their propulsion and actuation under the influence of an applied magnetic field.[27] Likewise, magneto-polymer composites have been reported for motile micromotors exhibiting the hyperthermia effect for possible usage in cancer treatment.[28–30] The applicability of micromotors[31–33] in the field of biomedicine is further promoted by the incorporation of biogenic materials which provide advanced functionalities[34,35] (like complex hierarchical structure, multifunctional surfaces with remarkable wetting, adhesive properties, etc.) with relatively low toxicity as compared to their synthetic counterparts.[36,37] These biogenic materials can be described as functional and structural components extracted from a natural source like plants (lectins as drug carriers),[38] bacteria (engineered outer membrane with vector properties),[39,40] mammalian cells (protein and cell-derived microvesicles),[41] etc. with distinct material properties.[42–48]

However, there is no study till date reporting micromotor activated surgery being performed at a single-cell level to highlight what can probably be the first step toward next-generation tools aiming at Feynman's futuristic vision of "swallowing the surgeon."[49] In this study, we present the first proof-of-concept for "dual-action microdaggers" where plant-derived biogenic micromotors exhibit dual functionality combining the surgeon's ability to create a cellular incision followed by the drug release feature facilitating highly localized drug administration. The drug release feature may be used to kill the harmful neighboring malignant cells (as shown in our study) or even to release supplementary medicine for the cells around to better compete against some infection. The loading of these calcified biotubes with the anticancer drug Camptothecin[50,51] allows for the site-specific activation of the drug in the acidic environment of HeLa cancer cells. This proof-of-concept study shows that our "dual-action" (cell-microdrilling and drug release) biogenic hybrid micromotor has the potential to perform noninvasive surgery with the precision to target a single cell together with the added advantage of the drug release feature to act as "cellular microsurgery with drug-rehabilitation" package.

We extracted calcified porous microneedles (40–60 µm long) from the *Dracaena* sp. plant[52,53] that possess drug carrier capability (much like calcium based drug carriers),[54–56] and coated these structures with a magnetic layer to facilitate cellular drilling by external magnetic actuation. It should be noted that such calcified biotubes are present in several plant species within specialized cells termed idioblasts and are scattered among both photosynthetic and nonphotosynthetic plant tissues.[57] **Figure 1**a shows a cross-section of the *Dracaenea marginata* leaf with the graphical representation of idioblast cells utilized for this research.

The calcified elongated porous structures with pointed ends are generally referred to as "raphides"[58] (see Figure 1b) and are primarily composed of calcium oxalate (CaO_x) and calcium carbonates. They play an important role in the maintenance of physiological functions like calcium regulation, plant defense, cellular detoxification, and tissue support.[59,60] The extraction of biogenic structures like raphides plays a crucial role because similar structures with comparable properties have never been produced in vitro regardless of the synthesis conditions.[61] Another major advantage of using biogenic materials is the fact that contrary to elaborate clean-room fabrication techniques,

Dr. S. K. Srivastava, Dr. M. Medina-Sánchez, Dr. B. Koch, Prof. O. G. Schmidt
Institute for Integrative Nanosciences
IFW Dresden
Helmholtzstraße 20, 01069 Dresden, Germany
E-mail: sarvesh.kumar@ifw-dresden.de

DOI: 10.1002/adma.201504327

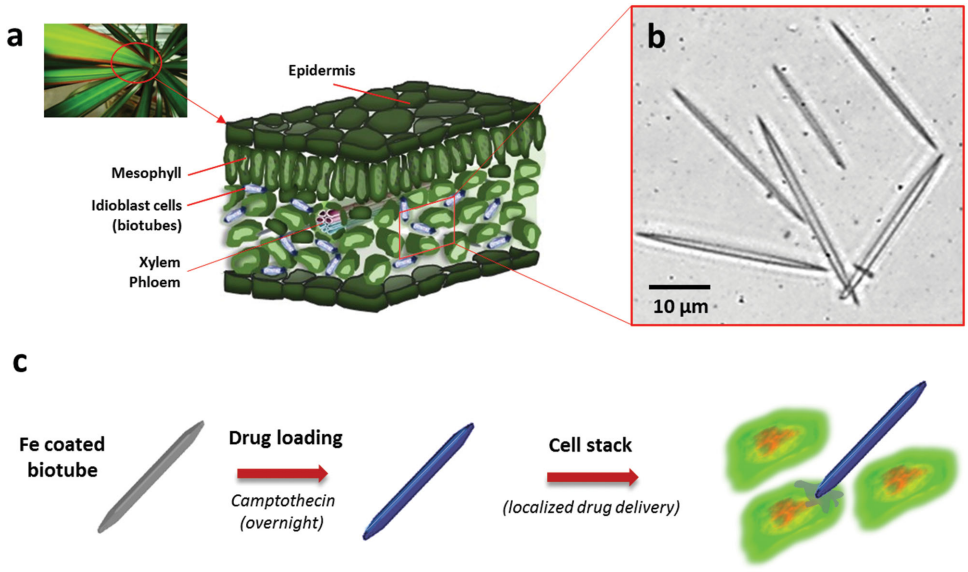

Figure 1. Schematics of biogenic microstructure extraction and the imparting of functional properties: a) *D. marginata* leaf with inset highlighting plant cell walls. b) Calcified biotubes (raphides) present in the idioblast cells. c) Schematic representation of imparting magnetic and drug delivery properties to the biotube.

a large amount of material can be obtained in relatively short time with minimal process control. We extracted these elongated porous structures to be utilized as a dual-action drug delivery unit with microdrilling capability as described in the Supporting Information. The calcified biotubes were coated with an Fe–Ti layer via an e-beam deposition process to incorporate magnetic control. Next, incubation with the drug Camptothecin for 3 d and subsequent purification steps conferred the dual-action capabilities (referred to as "microdaggers") as highlighted in Figure 1c. **Figure 2**a shows a large quantity of extracted biotubes which were subsequently utilized for this study.

The surface of the purified biotube structures was analyzed by an XPS study as shown in Figure 2b. The obtained spectra showed characteristic peaks for carbon, calcium (overlapping with carbon), and oxygen along with the absence of impurities over the biotube surface. The C1s peak for carbon at 288 eV shows the presence of an oxygenated framework with an O1s peak at ≈510 eV. Interesting structural features were observed by scanning electon microscopy (SEM) imaging as depicted in

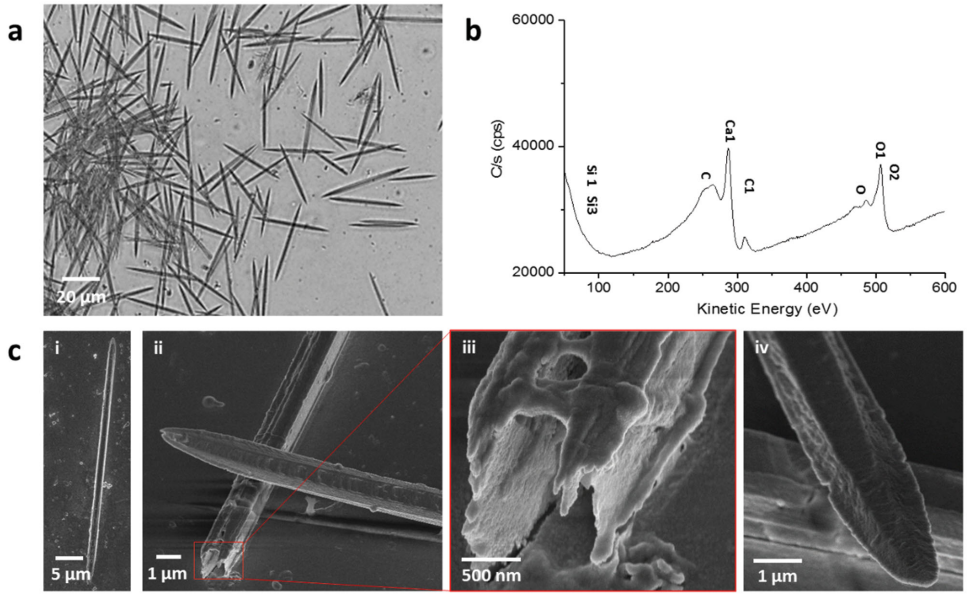

Figure 2. Material characterization of biotubes: a) optical microscope image showing extracted calcified biotubes. b) XPS spectra of the unmodified biotube surface. c) SEM images showing (i) single biotube, (ii) surface of the biotubes with structural break, (iii) inset highlighting internal cavity inside the porous biotube, and (iv) edged running along the biotube.

Adv. Mater. **2015**,
DOI: 10.1002/adma.201504327

Figure 2c. The calcified biotubes were ≈60 µm in length and 2.5 µm in width as shown in Figure 2c (i). We observe a distinct polygonal surface arrangement of the biotubes as highlighted in Figure 2c (ii) exhibiting a structural break in one of the tubes. This break is magnified in Figure 2c (iii) revealing a hollow space in the middle of these calcified microstructures with an internal cavity ≈0.8 µm^2 in area, capable of ferrying drug/particles inside. Another interesting feature for the drilling activity under magnetic actuation can be observed in Figure 2c (iv). We identified distinct edges (much like a broadsword) along the sides of the biotube constituting an ideal geometry for stabbing or piercing of cells (see Video S1 in the Supporting Information). Therefore, we see that the unique chemical and structural features offered by these calcified biotubes enable their application for subsequent cellular drilling and drug release.

Cellular drilling of HeLa cells is demonstrated with the Fe–Ti-coated biotubes under the influence of an external rotating magnetic field. We note that one structure is moving under the magnetic field, but the other is not moving at all. This happens because these biotubes tend to aggregate upon being deposited on a glass substrate prior to e-beam deposition resulting in limited Fe–Ti coating on the surface on some of the biotubes. Also, since our microdaggers are biogenic (plant derived), at times the Ti–Fe layer does not adhere perfectly all across the surface thereby restricting magnetic actuation. Therefore, while the majority of biotubes are magnetically actuated, a few may not show similar behavior.

Figure 3a depicts an angular frequency study of the Fe–Ti-coated biotubes in water and cell culture medium, respectively.

In both cases, we observed that upon increasing the frequency of the magnetic field, the magnetically actuated biotube adjusted its rotation from horizontal to vertical along its axis, thereby shifting from rotating parallel to the substrate to vertically standing[16] (Figure 3a inset), facilitating a stabbing/drill-like action. In Figure 3a, at the applied magnetic angular frequency of 500 rpm, we observed that the magnetically actuated biotube changes its orientation from horizontal to that of a vertical position allowing greater maneuvering around the target cell (see Video S4 in the Supporting Information). We achieved full vertical orientation (stand-up/drill-like position) for the biotubes at 800 rpm in both liquids.[62] Upon initiation of the drill-like motion in the presence of HeLa cells in cell culture medium, we observed the stabbing of biotubes into the cellular membrane resulting in cell death as confirmed by LIVE/DEAD cell viability test as shown in Figures 3b,c (see Video S2 in the Supporting Information). The nucleic acid stain SYBR Green was employed to label all cells with green fluorescence, while the red fluorescence of the membrane-impermeant dye Prodidium iodide (PI) was only observed in dead cells with a ruptured cell membrane.[63,64] Figure 3b shows our microdaggers in the vicinity of HeLa cells which display no red PI fluorescence highlighting that the cells are alive with intact cellular membranes. Upon magnetic actuation, the microdaggger initiates a drill-like motion around the target cell (highlighted by a dashed circle, see Video S2 in the Supporting Information) and successfully drills into the target cell by rupturing its cellular membrane. Thereby the PI dye is able to enter the ruptured cell and counterstain it red as shown in Figure 3c. Also, as observed in the video data (Video 2, Supporting Information), the moment the microdagger ruptures the cellular membrane of the target cell, it becomes locked/jammed by the cell. This is expected primarily for the reason that upon rupturing the cell, the viscous intracellular microenvironment increases the inertial force at the tip of the microdagger which can be

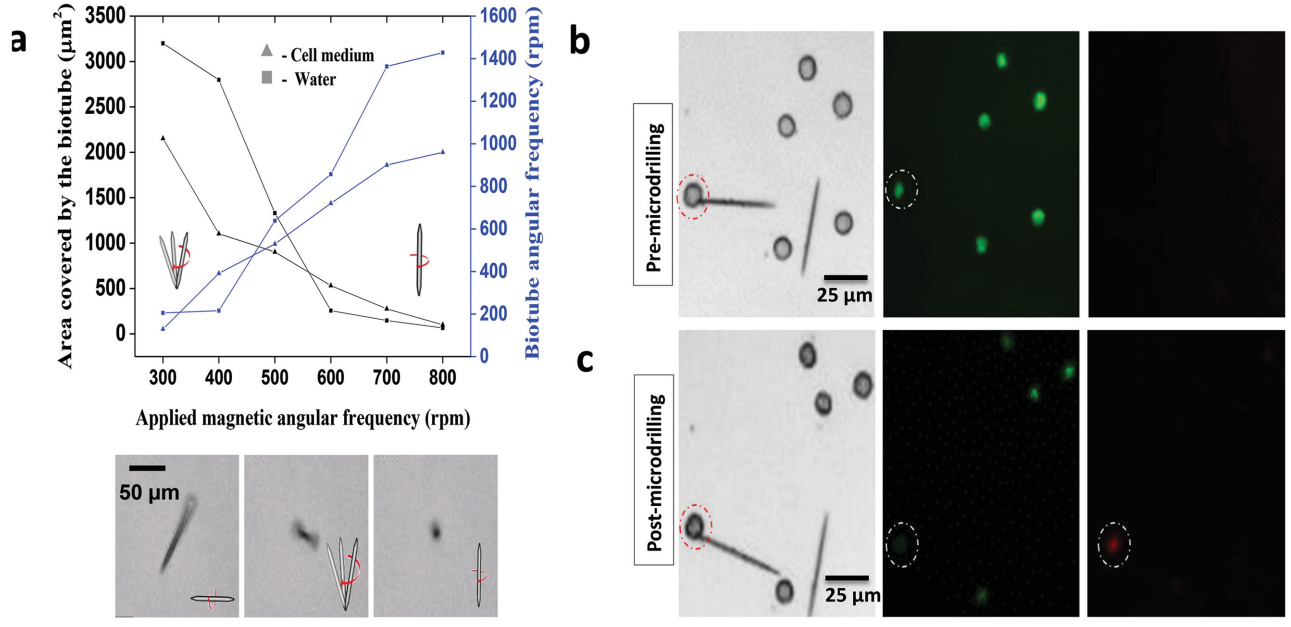

Figure 3. Magnetic control of biotube microdrillers: a) biotube angular frequency (rpm) and covered area in comparison to the applied magnetic angular frequency (rpm). Note that the blue color highlights biotube angular frequency while black denotes the area covered by that biotube. b,c) Brightfield and fluorescence images of HeLa cells b) before and c) after microdrilling. The target cell is highlighted by a dotted circle. Live cells display green and dead cells additionally red fluorescence. Note that a slight rearrangement of the cells before and after the drilling is normal due to the flow generated by the rotation of the microdagger (see Video S2 in the Supporting Information).

clearly understood by the difference in dynamic viscosity of water (1 cP) to that of a cell (150–250 cP).[65] Another significant reason can be the rapid cellular response to attempt resealing of the ruptured membrane as reported by Terasaki et al.[66–68] "Living, nucleated cells respond to microneedle punctures of their plasma membranes by rapidly (within second) resealing the breach created. The mechanism used is Ca^{2+} dependent and hypothesized to be an active process governed by specific protein–protein interactions that result in a local exocytotic reaction. As a result of this exocytotic response, new membrane is added locally to the site of cell surface injury."

Finally, these microdaggers were loaded with the anticancer drug Camptothecin to study the associated drug-release effect of these biotubes. We chose Camptothecin as a model drug due to its known anticancer activity, with two of its derivatives already being approved for cancer treatment,[69,70] and its low solubility in aqueous environments. Additionally, it exists in two distinguishable forms: the inactive carboxylate form at physiological pH and the active lactone form at acidic pH (pH 5-6).[71] While the physiological pH of healthy tissue is usually estimated to be slightly basic (around pH 7.5), the microenvironment of most tumors can be more acidic (pH 5.8-7.6),[72] e.g., due to an increased production of lactic acid.[73,74] In this study, we exploited this feature of tumor tissue to selectively activate the effective lactone form of Camptothecin. This also provides an inherent advantage over the traditional drug carriers as we can fuse the dual functionality of magnetic control (microdrilling) with that of the drug vector (see Video S3 in the Supporting Information) thereby limiting the inadvertent side effects on healthy tissue by site-specific delivery. Detailed information about the experimental conditions and setup assembly can be found in the Supporting Information.

To demonstrate the same, fluorescently labeled human HeLa cervical cancer cells were incubated with the Camptothecin-loaded microdaggers for up to 3 d. The Camptothecin loading can be nicely visualized due to the blue autofluorescence upon UV excitation (Figure S1, Supporting Information). The HeLa cells expressed GFP-tubulin and histone H2B-mCherry, labeling the cell cytoskeleton with green and the cell nuclei with red fluorescence. In **Figure 4**, brightfield as well as fluorescence images of HeLa cells are shown that depict the cell growth in the presence of control and drug-loaded biotubes. Over the course of 3 d, the HeLa cells of the control experiment proliferated actively until forming a dense and tightly packed cell monolayer. This demonstrated the general biocompatibility of the biotube material. Occasionally, we observed localized cell rupturing through unloaded biotubes thereby emphasizing the penetration potential of these biotubes. In the presence of the

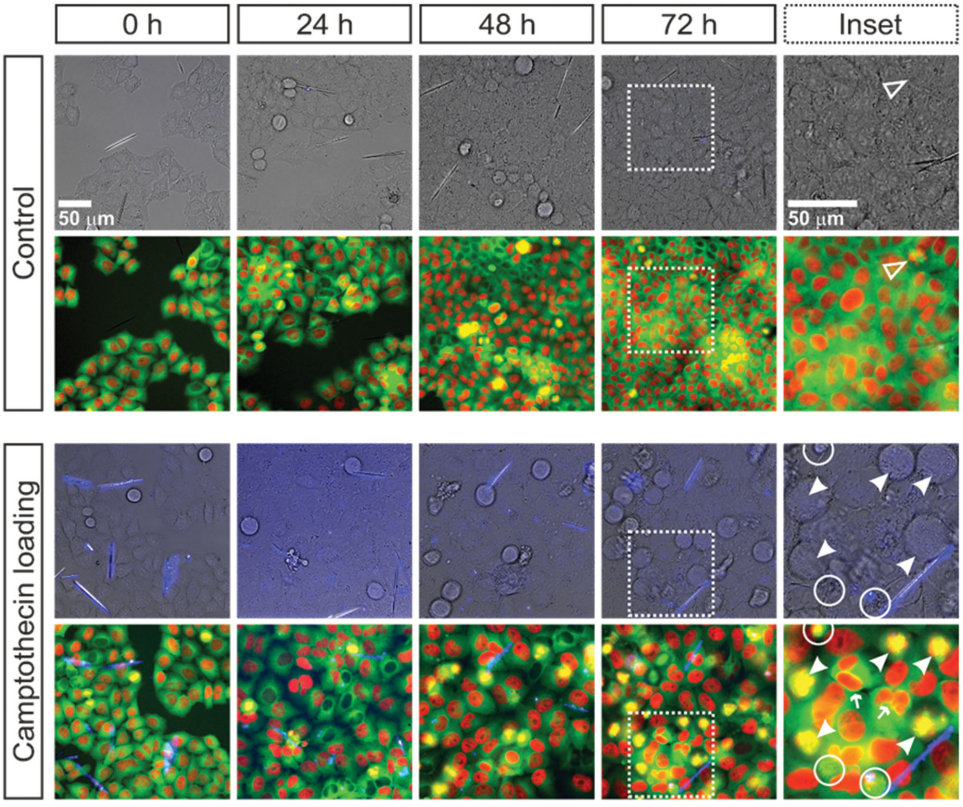

Figure 4. Drug administration via biotubes. HeLa cells are incubated with the unmodified (control) and camptothecin-loaded biotubes for 3 d. For each condition and time point indicated at the top, a DIC (differential interference contrast) image overlayed with the blue drug autofluorescence, as well as a fluorescence image visualizing the cell cytoskeleton (green), cell nuclei (red), and drug autofluorescence (blue) are shown. For the 72 h time point, parts of the images (indicated by dotted white squares) are magnified in the very right panels. Here, the open arrow head points at a proper cell division, whereas filled arrow heads indicate dividing cells with a defective assembly of the mitotic spindle (e.g., tripolar). Small arrows point at cells with two nuclei, and white circles highlight dead cells. The scale bars equal 50 μm.

Adv. Mater. **2015**,
DOI: 10.1002/adma.201504327

drug-loaded microdaggers, the cell layer grew strikingly less dense and after 24 h already aberrant cell divisions (in Figure 4, cells highlighted by filled arrow heads) characterized by, e.g., tripolar mitotic spindles in cells rounded for division occurred. The round aberrant cell morphologies accumulated over time, indicating that the HeLa cells could no longer properly divide and were caught in mitosis.[75,76] Additionally, dead cells were present in these samples (see Figure 4, cells highlighted by white circles). Therefore, the Camptothecin transmitted via the biotube carrier did remarkably reduce HeLa cell proliferation and facilitated cell death. This unique combination of single-cell microsurgery with drug release capability has the potential to explore similar porous inorganic/biogenic materials as a new class of drug delivery/cell-manipulation and hybrid micromotor system in the near future.

In conclusion, we presented a next generation concept for "microsurgery with drug rehabilitation" feature where cancerous/infected cells can be targeted followed by drug-release (like anticancer or supplementary medication). The ability of the microdagger to drill into a single cell can also be used as an anchoring mechanism to dock them for subsequent release of drug in case of other drug mediated secondary treatments. This dual-functionality of creating cellular incision together with site-directed drug delivery will significantly reduce lateral health damages associated with treatment regimens like that of chemotherapy among others. Finally, the future of such "medi-bots" will be greatly influenced by their choice of propulsion medium (harnessing power from the in vivo environment), ability to provide target specific signals (microsensors) or real-time imaging modalities and high-volume powering with robust controlling system.

Supporting Information

Supporting Information is available from the Wiley Online Library or from the author.

Acknowledgements

S.K.S. would like to thank Deutscher Akademischer Austauschdienst (DAAD)-Leibniz for funding. The authors thank Dr. Steffen Oswald for XPS analysis, Dr. Stefan Baunack and Dr. Matthew Jorgensen for SEM analysis and Franziska Hebenstreit for the culturing of HeLa cells.

Received: September 3, 2015
Revised: October 7, 2015
Published online:

[1] S. Yao, Y. Shu, Y.-J. Yang, X. Yu, D.-W. Pang, Z.-L. Zhang, *Chem. Commun.* **2013**, *49*, 7114.
[2] M. Toner, H. Buettner, *Biotechnol. Prog.* **1998**, *14*, 355.
[3] D. A. LaVan, D. M. Lynn, R. Langer, *Nat. Rev. Drug Discov.* **2002**, *1*, 77.
[4] R. Fernandes, D. H. Gracias, *Adv. Drug Deliv. Rev.* **2012**, *64*, 1579.
[5] A. Sen, D. Patra, S. Sengupta, W. Duan, H. Zhang, R. Pavlick, *Nanoscale* **2013**, *5*, 1273.
[6] R. C. McGlennen, *Clin. Chem.* **2001**, *47*, 393.
[7] G. W. Rogers, *AIP Conf. Proc.* **2012**, *1433*, 705.
[8] B. J. Nelson, I. K. Kaliakatsos, J. J. Abbott, *Annu. Rev. Biomed. Eng.* **2010**, *12*, 55.
[9] J. P. Desai, A. Pillarisetti, A. D. Brooks, *Annu. Rev. Biomed. Eng.* **2007**, *9*, 35.
[10] Y. Yamanishi, Y. C. Lin, F. Arai, presented at *IEEE Int. Conf. Intell. Robot. Syst.*, **2007**, San Diego, CA, USA, Oct 29 – Nov 2, p. 753.
[11] W. Gao, R. Dong, S. Thamphiwatana, J. Li, W. Gao, L. Zhang, J. Wang, *ACS Nano* **2015**, *9*, 117.
[12] E. Morales-Narváez, M. Guix, M. Medina-Sánchez, C. C. Mayorga-Martinez, A. Merkoçi, *Small* **2014**, *10*, 2542.
[13] S. Balasubramanian, D. Kagan, C. M. Jack Hu, S. Campuzano, M. J. Lobo-Castañon, N. Lim, D. Y. Kang, M. Zimmerman, L. Zhang, J. Wang, *Angew. Chem. Int. Ed.* **2011**, *50*, 4161.
[14] F. Mou, C. Chen, Q. Zhong, Y. Yin, H. Ma, J. Guan, *ACS Appl. Mater. Interfaces* **2014**, *6*, 9897.
[15] A. A. Solovev, W. Xi, D. H. Gracias, S. M. Harazim, C. Deneke, S. Sanchez, O. G. Schmidt, *ACS Nano* **2012**, *6*, 1751.
[16] W. Xi, A. Solovev, A. N. Ananth, D. Gracias, S. Sanchez, O. G. Schmidt, *Nanoscale* **2013**, *5*, 1294.
[17] W. Hu, K. S. Ishii, Q. Fan, A. T. Ohta, *Lab Chip* **2012**, *12*, 3821.
[18] M. P. Kummer, J. J. Abbott, B. E. Kratochvil, R. Borer, A. Sengul, B. J. Nelson, *IEEE Trans. Robot.* **2010**, *26*, 1006.
[19] G. Dogangil, O. Ergeneman, J. J. Abbott, S. Pané, H. Hall, S. Muntwyler, B. J. Nelson, presented at *2008 IEEE/RSJ Int. Conf. Intell. Robot. Syst. IROS* 2008, Nice, France, Sep 22 – 26, p. 1921.
[20] E. Gultepe, J. S. Randhawa, S. Kadam, S. Yamanaka, F. M. Selaru, E. J. Shin, A. N. Kalloo, D. H. Gracias, *Adv. Mater.* **2013**, *25*, 514.
[21] K. E. Peyer, L. Zhang, B. J. Nelson, *Nanoscale* **2013**, *5*, 1259.
[22] E. D. Diller, M. Sitti, *Found. Trends Robot.* **2011**, *2*, 143.
[23] P. Dario, M. C. Carrozza, A. Benvenuto, A. Menciassi, *J. Micromech. Microeng.* **2000**, *10*, 235.
[24] D. B. Camarillo, T. M. Krummel, J. K. Salisbury, *Am. J. Surg.* **2004**, *188*, 2S.
[25] C. Bergeles, G.-Z. Yang, *IEEE Trans. Biomed. Eng.* **2014**, *61*, 1565.
[26] J. J. Abbott, K. E. Peyer, L. X. Dong, B. J. Nelson, *Springer Tracts Adv. Robot.* **2010**, *66*, 157.
[27] M. Feldmann, S. Büttgenbach, *IEEE Trans. Magn.* **2007**, *43*, 3891.
[28] J. Nunes, K. P. Herlihy, L. Mair, R. Superfine, J. M. Desimone, *Nano Lett.* **2010**, *10*, 1113.
[29] P. L. Venugopalan, R. Sai, Y. Chandorkar, B. Basu, S. Shivashankar, A. Ghosh, *Nano Lett.* **2014**, *14*, 1968.
[30] L. Zhang, J. J. Abbott, L. Dong, B. E. Kratochvil, D. Bell, B. J. Nelson, *Appl. Phys. Lett.* **2009**, *94*, 64107.
[31] S. Sanchez, A. A. Solovev, S. Schulze, O. G. Schmidt, *Chem. Commun.* **2011**, *47*, 698.
[32] S. Sundararajan, P. E. Lammert, A. W. Zudans, V. H. Crespi, A. Sen, *Nano Lett.* **2008**, *8*, 1271.
[33] Z. Wu, T. Li, J. Li, W. Gao, T. Xu, C. Christianson, W. Gao, M. Galarnyk, Q. He, L. Zhang, J. Wang, *ACS Nano* **2014**, *8*, 12041.
[34] C. Sanchez, H. Arribart, M. M. G. Guille, *Nat. Mater.* **2005**, *4*, 277.
[35] K. Liu, L. Jiang, *ACS Nano* **2011**, *5*, 6786.
[36] Q. Wang, X. Zhuang, J. Mu, Z.-B. Deng, H. Jiang, L. Zhang, X. Xiang, B. Wang, J. Yan, D. Miller, H.-G. Zhang, *Nat. Commun.* **2013**, *4*, 1867.
[37] N. Roveri, B. Palazzo, M. Iafisco, *Expert Opin. Drug Deliv.* **2008**, *5*, 861.
[38] C. M. Lehr, *J. Control. Release* **2000**, *65*, 19.
[39] V. Gujrati, S. Kim, S. H. Kim, J. J. Min, H. E. Choy, S. C. Kim, S. Jon, *ACS Nano* **2014**, *8*, 1525.
[40] S. K. Srivastava, M. Constanti, *J. Nanoparticle Res.* **2012**, *14*, 831.
[41] F. Lienert, J. J. Lohmueller, A. Garg, P. a Silver, *Nat. Rev. Mol. Cell Biol.* **2014**, *15*, 95.
[42] M. Sumper, E. Brunner, *Adv. Funct. Mater.* **2006**, *16*, 17.

[43] S. Srivastava, C. Ogino, A. Kondo, *Green Process. Nanotechnol. SE-8* (Eds: V. A. Basiuk, E. V Basiuk), Springer International Publishing Switzerland **2015**, p. 237.
[44] S. K. Srivastava, R. Yamada, C. Ogino, A. Kondo, *Carbon* **2013**, *56*, 309.
[45] S. K. Srivastava, J. S. del Rio, C. K. O'Sullivan, C. Ogino, A. Kondo, *RSC Adv.* **2014**, *4*, 48458.
[46] P. B. Malafaya, G. A. Silva, R. L. Reis, *Adv. Drug Deliv. Rev.* **2007**, *59*, 207.
[47] K. Kamata, S. Suzuki, M. Ohtsuka, M. Nakagawa, T. Iyoda, A. Yamada, *Adv. Mater.* **2011**, *23*, 5509.
[48] W. Gao, X. Feng, A. Pei, C. R. Kane, R. Tam, C. Hennessy, J. Wang, *Nano Lett.* **2014**, *14*, 305.
[49] R. P. Feynman, *Eng. Sci.* **1960**, *23*, 22.
[50] Y. Pommier, C. Marchand, *Nat. Rev. Drug Discov.* **2012**, *11*, 250.
[51] E.-H. Liu, L.-W. Qi, Q. Wu, Y.-B. Peng, P. Li, *Mini Rev. Med. Chem.* **2009**, *9*, 1547.
[52] S. V. Pennisi, D. B. McConnell, L. B. Gower, M. E. Kane, T. Lucansky, *New Phytol.* **2001**, *150*, 111.
[53] X. Li, D. Zhang, V. J. Lynch-Holm, T. W. Okita, V. R. Franceschi, *Plant Physiol.* **2003**, *133*, 549.
[54] X. Ma, L. Li, L. Yang, C. Su, Y. Guo, K. Jiang, *Mater. Lett.* **2011**, *65*, 3176.
[55] W. Wei, G.-H. Ma, G. Hu, D. Yu, T. Mcleish, Z.-G. Su, Z.-Y. Shen, *J. Am. Chem. Soc.* **2008**, *130*, 15808.
[56] K. F. Mueller, S. J. Heiber, *Crosslinked*, CA1225030, **1985**.
[57] A. S. Foster, *Protoplasma* **1956**, *46*, 184.
[58] S. G. Pritchard, S. A. Prior, H. H. Rogers, C. M. Peterson, *Int. J. Plant Sci.* **2000**, *161*, 917.
[59] P. A. Nakata, *Plant Sci.* **2003**, *164*, 901.
[60] V. R. Franceschi, H. T. Horner, *Bot. Rev.* **1980**, *46*, 361.
[61] V. R. Franceschi, P. A. Nakata, *Annu. Rev. Plant Biol.* **2005**, *56*, 41.
[62] P. Dhar, C. D. Swayne, T. M. Fischer, T. Kline, A. Sen, *Nano Lett.* **2007**, *7*, 1010.
[63] P. Soudant, F. L. E. Chu, E. D. Lund, *J. Eukaryot. Microbiol.* **2005**, *52*, 492.
[64] T. Suzuki, K. Fujikura, T. Higashiyama, K. Takata, *J. Histochem. Cytochem.* **1997**, *45*, 49.
[65] M. K. Kuimova, *Phys. Chem. Chem. Phys.* **2012**, *14*, 12671.
[66] M. Terasaki, K. Miyake, P. L. McNeil, *J. Cell Biol.* **1997**, *139*, 63.
[67] P. L. McNeil, R. A. Steinhardt, *J. Cell Biol.* **1997**, *137*, 1.
[68] A. Rodríguez, P. Webster, J. Ortego, N. W. Andrews, *J. Cell Biol.* **1997**, *137*, 93.
[69] B. L. Staker, K. Hjerrild, M. D. Feese, C. A. Behnke, A. B. Burgin, L. Stewart, *Proc. Natl. Acad. Sci. USA* **2002**, *99*, 15387.
[70] Y. Pommier, *Nat. Rev. Cancer* **2006**, *6*, 789.
[71] J. Fassberg, V. J. Stella, *J. Pharm. Sci.* **1992**, *81*, 676.
[72] I. F. Tannock, D. Rotin, *Cancer Res.* **1989**, *49*, 4373.
[73] Y. Kato, S. Ozawa, C. Miyamoto, Y. Maehata, A. Suzuki, T. Maeda, Y. Baba, *Cancer Cell Int.* **2013**, *13*, 89.
[74] M. F. McCarty, J. Whitaker, *Altern. Med. Rev.* **2010**, *15*, 264.
[75] B. A. A. Weaver, D. W. Cleveland, *Cancer Cell* **2005**, *8*, 7.
[76] P. M. Kubara, S. Kernéis-Golsteyn, A. Studény, B. B. Lanser, L. Meijer, R. M. Golsteyn, *Biochem. J.* **2012**, *446*, 373.

Adv. Mater. **2015**,
DOI: 10.1002/adma.201504327